EAI Endorsed Transactions
on Sustainable Manufacturing and Renewable Energy Research Article EAI.EU

Stabilization of a Cart-Pendulum System Using the Pole Placement Technique

Q.K.M. Bui[1], H.N. Nguyen[1], T.T. Duong[1*]

[1]Department of Mechatronics, Faculty of Mechanical Engineering, Ho Chi Minh City

University of Technology (HCMUT), 268 Ly Thuong Kiet, Dien Hong Ward, Ho Chi Minh City, Viet Nam

Abstract

This study addresses the stabilization of the Cart Inverted Pendulum (CIP), a system widely recognized as a foundational challenge in control theory because of its unstable, nonlinear, and under controlled properties. Achieving stability in the CIP is essential for developing control methods for modern applications like robotics. This paper implements the Pole Placement method to ensure the system remains stable. The method begins by linearizing the nonlinear system dynamics about the unstable vertical configuration and expressing them in a state-variable form. After confirming the system's controllability, a state-feedback controller is designed by strategically assigning closed-loop pole locations. This placement dictates the system's performance, allowing for specific targets for damping and setting time. The controller's effectiveness is demonstrated through numerical simulations in MATLAB/Simulink, which confirm the system's successful transition from instability to stable, regulated control of both the angle of pendulum and the position of cart. This analysis also illuminates the essential trade-off between the system's response speed and the required energy control. The work ultimately affirms that Pole Placement is a highly effective, understandable, and computationally practical technique for stabilizing complex underactuated systems.

Keywords: Cart Inverted Pendulum, Pole Placement Control, State-Feedback Control, Linearization, Underactuated Systems, MATLAB Simulation.

Received on 27 November 2025, accepted on 05 January 2026, published on 14 January 2026

doi: 10.4108/eetsmre.11143

*Corresponding author. Email: dttrung.sdh242@hcmut.edu.vn

1. Introduction

The CIP system stands as a canonical benchmark problem for validating such control strategies. Moreover, the CIP system has numerous practical applications including self-balancing vehicles such as Segways, robotic manipulators, and aerial drones all share dynamic characteristics with the CIP. As a typical example of an underactuated, unstable, and nonlinear system, it perfectly describes the core challenges of modern control engineering. Implementing pole placement control for the CIP system begins with verifying the controllability of the linearized model. If the system is controllable, one can select desired pole locations based on performance criteria, such as a fast but stable response, minimal overshoot, and limited control effort. The feedback gain matrix is computed accordingly, ensuring that the closed-loop poles match the predefined specifications. One significant advantage of this method is its flexibility: designers can easily adjust pole locations to tune the transient response without re-deriving the control law from first principles [16]. Additionally, Numerical simulation plays a crucial role in validating the pole placement design. Simulation software such as MATLAB/Simulink are typically used to model the nonlinear CIP dynamics and simulate the system's behaviors under various control configurations [17]. Through simulation, one can compare the system's open-loop instability with its closed-loop stability after pole placement. Generally, demonstrate that as the poles are placed farther left in the complex plane, the system responds faster but with increased overshoot and control effort. Therefore, a trade-off exists between stability margins, speed of response, and energy efficiency. The pole placement method allows fine-tuning of these trade-offs, leading to improved overall system performance when properly designed [18].

This paper focuses on stabilizing a cart inverted pendulum (CIP) by first linearizing its model and then designing a pole placement controller. The success of this stabilization approach is demonstrated through MATLAB-based simulations.

2. Literature review

The CIP system serves as a basic test case in control engineering because whose independent coordinates outnumber its actuation channels, behaves in a nonlinear way and is naturally unstable. On that account researchers have created many control schemes to keep it upright, from traditional linear methods to recent data-based methods. This section surveys those schemes to explain why the present work chose Pole Placement.

Linear control methods stay popular because they run fast and their stability is proven. Many papers compare Linear Quadratic Regulators (LQR) plus Linear Quadratic Gaussian (LQG) with ordinary PID controllers. Tests show that LQG gives quick response and stays stable - yet LQR usually works better when noise is present [19]. Extended LQG but also similar variants serve in situations with few sensors, but they need nonlinear models of higher order, which raises complexity [20]. Among linear techniques, Pole Placement through state feedback is direct - the designer fixes the closed loop pole positions to obtain the wanted damping and settling time [25]. The drawback is that the chosen poles fix the required control energy - a clear trade off study is essential [25].

Advanced model-based approaches, such as Sliding Mode Control (SMC) and Model Predictive Control (MPC), have been extensively studied to overcome the drawbacks of linear approximations. The ability of MPC to manage system restrictions and trajectory tracking is particularly well known. Comparative studies between real-time MPC and LQR on rotary pendulums demonstrate that, although MPC handles constraints better, it struggles with sampling noise and severe computational demands on embedded hardware [21]. Integrating model refinement procedures to increase prediction accuracy is one way that MPC is being improved [27]. In a similar vein, strong control techniques like worst-case optimization and Bayesian control have been put out as a means of dealing with sensor uncertainty and perturbations [23] [28]. Additionally, hierarchical sliding mode control (HSMC) coupled with optimization methods has been demonstrated to lessen the "chattering" effect frequently seen in robust control, resulting in superior performance when compared to standard SMC or LQR [22] [33].

The use of Reinforcement Learning (RL) and Machine Learning (ML) in the CIP system is a quickly expanding trend in contemporary literature. These techniques seek to infer control rules straight from data. Reinforcement learning methods like Q-learning and Deep Q-Networks have shown the potential to swing up and stabilize pendulums, sometimes outperforming PID and LQR measures [29] [31]. To make use of big data for controller tuning, more complex frameworks combine RL with MPC [26], or they use "Sim-to-Real" transfer to close the gap between simulation and physical hardware [24]. But compared to traditional physics-based models, these techniques frequently have significant implementation complexity, instability during the training process, and a lack of transparency [32] [34].

Although sophisticated nonlinear and learning-based controllers can perform well in certain situations, they usually have high computational costs and are difficult to implement. On the other hand, the Pole Placement technique provides a straightforward and computationally efficient approach that is excellent for comprehending the system's underlying dynamics [12]. Even with the introduction of modern algorithms, Pole Placement is still a potent method for archiving a balance between response speed and energy efficiency.

3. The proposed approach

3.1. System Modelling

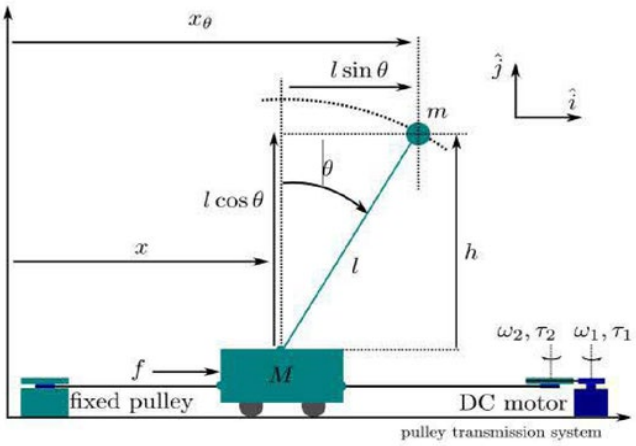

Fig.1. The cart inverted pendulum

Fig 1 illustrates the cart inverted pendulum system. A DC motor is used to move the cart along x-axis direction. The mechanical transmission using belt and pulley is used to gain the actuator torque. The velocity and the acceleration of the cart are controlled by controlling the angular velocity and acceleration of the DC motor.[36]

A. *Mathematical Model of the CIP*

A mathematical model of the cart inverted pendulum should be derived to map the system input (the force applied to cart, f) to the system output (x, θ). In a mathematical notation, the mapping can be expressed as $f \in \mathbb{R}^1 \mapsto (x, \theta) \in \mathbb{R}^2$. In this work, Lagrange's Equation is used to describe the system model. The basic

tenet of Lagrange's equation is the description of the system by one of equalised coordinate $q = \{q_1, \cdots, q_i, \cdots, q_n\}$, where $n$is the total assigned equalised coordinate. $q_i$is a free degree of freedom of true system which totally combine the constraints unique to that system, i.e., the communication among parts of the system. The Lagrangian equation $\mathcal{L}$ is declared by the potential energy $P$and the kinetic energy Kas explained as

$$\mathcal{L} = \mathcal{K}(\mathbf{q}, \dot{\mathbf{q}}) - \mathcal{P}(\mathbf{q}) \quad (1)$$

where q = [x, θ] is the vector of equalized coordinate and q˙ is the derivation of it, $\mathcal{K}$ is the total of the system's kinetic energy and $\mathcal{P}$ is the system's potential energy. In this inverted pendulum system, the kinetic energy is governed by two factors including the kinetic energy of the cart, $\mathcal{K}_M$, as well as the kinetic energy of the pendulum, $\mathcal{K}_m$, which are respectively presented:

$$\mathcal{K}_M = \frac{1}{2}M\dot{x}^2 \quad (2)$$

$$\mathcal{K}_m = \frac{1}{2}m(\dot{x}_\theta + \dot{h}) \quad (3)$$

where M is the cart mass, x˙ is the cart's linear velocity, m is the pendulum mass, x˙θ is the rate of the pendulum position following to the horizontal axis and h˙ is the rate of the pendulum position on the vertical axis. Based on Fig. 1, the total kinetic energy of the system is derived

$$\begin{aligned} \mathcal{K} &= \mathcal{K}_M + \mathcal{K}_m \\ &= \frac{1}{2}M\dot{x}^2 + \frac{1}{2}m(\dot{x}^2 + 2\dot{x}l\dot{\theta}\cos\theta + l^2\dot{\theta}^2) \end{aligned} \quad (4)$$

On the other hand, the potential energy is directly affected by the mass of the pendulum m, which is presented as

$$\begin{aligned} \mathcal{P} &= mgh \\ &= mgl\cos\theta \end{aligned} \quad (5)$$

In general, the Eq. (1) can be rewritten with the subcomponents from Eq. (2) to Eq. (5) as follows:

$$\begin{aligned} \mathcal{L} &= \frac{1}{2}M\dot{x}^2 + \frac{1}{2}m(\dot{x}^2 + 2\dot{x}l\dot{\theta}\cos\theta + l^2\dot{\theta}^2) \\ &\quad -mgl\cos\theta \end{aligned} \quad (6)$$

In terms of x and θ, the derivatives of the Eq. (1) following to x and θ are respectively derived:

$$\frac{\mathrm{d}}{\mathrm{d}t}\left(\frac{\partial\mathcal{L}}{\partial\dot{x}}\right) - \frac{\partial\mathcal{L}}{\partial x} = f \quad (7)$$

$$\frac{\mathrm{d}}{\mathrm{d}t}\left(\frac{\partial\mathcal{L}}{\partial\dot{\theta}}\right) - \frac{\partial\mathcal{L}}{\partial\theta} = 0 \quad (8)$$

Deriving for each term in the differential equation in Eq. (7) and Eq. (8), it can be obtained that

$$\frac{\partial\mathcal{L}}{\partial\dot{x}} = (m+M)\dot{x} + ml\dot{\theta}\cos\theta \quad (9)$$

$$\frac{\mathrm{d}}{\mathrm{d}t}\left(\frac{\partial\mathcal{L}}{\partial\dot{x}}\right) = (m+M)\ddot{x} + ml(\ddot{\theta}\cos\theta - \dot{\theta}^2\sin\theta) \quad (10)$$

$$\frac{\partial\mathcal{L}}{\partial x} = 0 \quad (11)$$

and

$$\frac{\partial\mathcal{L}}{\partial\dot{\theta}} = ml\dot{x}\cos\theta + ml^2\dot{\theta} \quad (12)$$

$$\frac{\mathrm{d}}{\mathrm{d}t}\left(\frac{\partial\mathcal{L}}{\partial\dot{\theta}}\right) = ml(\ddot{x}\cos\theta - \dot{\theta}\dot{x}\sin\theta) + ml^2\ddot{\theta} \quad (13)$$

$$\frac{\partial\mathcal{L}}{\partial\theta} = -m\dot{x}l\dot{\theta}\sin\theta + mgl\sin\theta \quad (14)$$

Substituting from Eq. (9) to Eq. (14) into Eq. (7) and Eq. (8), the dynamics model of the inverted pendulum system is declared as follows

$$f = (M+m)\ddot{x} + ml\ddot{\theta} \quad (15)$$

$$0 = \ddot{x} + l\ddot{\theta} - g\theta \quad (16)$$

From Eq. (15) and Eq. (16), it is noted that the existence of those non-linear components sin(), cos(), $\theta^{\cdot 2}$, leading to the nonlinearity of the inverted pendulum system.

Assumption 1. To linearize the system, it is assumed that the pendulum rotates near around the equilibrium (θ≈0). As a result, it can be approximated that $\sin\theta \approx \theta$, $\cos\theta \approx 1$, $\theta^{\cdot 2} \approx 0$, $\dot{\theta}$ and $\dot{\theta}\theta = 0$.

B. DC Motor: Torque, Armature Voltage, and Angular Velocity of this model

The DC motor armature circuit equation can be calculated using Kirchhoff's voltage law:

$$i_a R_a + L_a\frac{\mathrm{d}i_a}{\mathrm{d}t} + v_b \models v_a \quad (17)$$

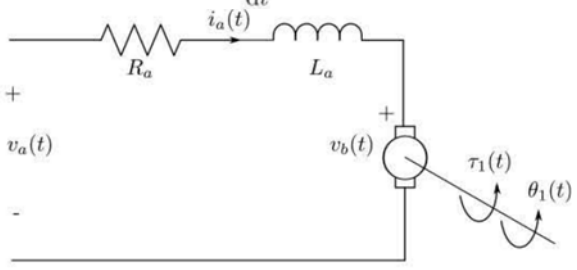

Fig. 2. DC Motor Armature Equivalent Circuit

The relation between generated back electromotive force (emf), *Vb,* and the rotational speed of the rotor is:

$$v_b = K_b\frac{\mathrm{d}\theta_1}{\mathrm{d}t} \quad (18)$$

where K_b is the back emf constant.

The torque of motor τ_1 is the output of the actuator that ultimately causes the force to move the cart.

$$\tau_1 = K_t i_a \quad (19)$$

where K_t is the motor torque constant.

The Eq. (20) is the expression of the DC motor armature circuit equation where the armature current and its derivative have been substituted by terms involving the motor torque and the motor angular velocity.

$$\frac{\tau_1}{K_t}R + L_a\frac{\mathrm{d}^2\tau_1}{(\mathrm{d}t)^2} + K_b\frac{\mathrm{d}\theta_1}{\mathrm{d}t} = v_a \quad (20)$$

Ignoring the motor inductance, the function of armature circuit can be simplified as:

$$\tau_1 = -K_t\frac{K_b}{R_a}\omega_1 + \frac{K_t}{R_a}v_a \quad (21)$$

The mechanical transmission ratio in the system can be calculated as:

$$\frac{\tau_2}{\tau_1} = \frac{N_2}{N_1} = \frac{\omega_1}{\omega_2} = \frac{r_2}{r_1} \quad (22)$$

where r is the radius of the pulley and N is the gear teeth number.

The relation between the motor angular velocity and the cart velocity $\dot{x}$ is

$$\frac{2\pi r_2}{\dot{x}} = \frac{r_2}{r_1}\frac{2\pi}{\omega_1} \quad (23)$$

Eq. (24) connects the rotational output of the motor to the linear movement of the cart. This allows the preceding electrical model to be expressed entirely in terms of the cart's mechanical state variables.

$$\omega_1 = \frac{\dot{x}}{r_1} \quad (24)$$

Combining Eq. (24) and Eq. (21), the Eq. (25) can be obtained as:

$$\tau_1 = K_r(-K_b\frac{\dot{x}}{r_1} + v_a) \quad (25)$$

The torque $\tau_2$causing the force that moves the cart, so, the transform is needed $\tau_1 \mapsto \tau_2$. Consequently, using $fr_2 = \tau_2$(the force that perpendicular to the direction of $r_2$from pulley centre), it can be verified that

$$f = \frac{K_r}{r_1}(-K_b\frac{\dot{x}}{r_1} + v_a) \quad (26)$$

where $K_r = \frac{K_t}{R_a}$. From Eq. (36) and Eq. (25), a new Lagrange's function in term of equalised coordinate $x$is declared as

$$\frac{K_r}{r_1}v_a = (M+m)\ddot{x} + \frac{K_rK_b}{(r_1)^2}\dot{x} + ml\ddot{\theta} \quad (27)$$

The following notions are used to simplify the derivation.

$$c_1 = \frac{K_rK_b}{(r_1)^2} \quad (28)$$

$$c_2 = \frac{K_r}{r_1} \quad (29)$$

from Eq. (27), and from the term $\theta^{\cdot\cdot}$ and Eq. (16) into Eq. (27), the first differential equation can be described as

$$\ddot{x} = \frac{1}{M}(c_2v_a - c_1\dot{x} - mg\theta) \quad (30)$$

From Eq. (16), the angular acceleration can be obtained as:

$$\ddot{\theta} = \frac{1}{l}(g\theta - \ddot{x}) \quad (31)$$

From Eq. (30) and Eq. (31), the second differential function of the system can be formed as

$$\ddot{\theta} = \frac{1}{l}\left(g\theta - \frac{1}{M}(c_2v_a - c_1\dot{x} - mg\theta)\right) \quad (32)$$

$$= -\frac{c_2}{Ml}v_a + \frac{c_1}{Ml}\dot{x} + \frac{(M+m)g}{Ml}\theta \quad (33)$$

Ultimately, the differential equations describing the cart-pendulum system were derived using Lagrange's method, while explicitly incorporating actuator dynamics into the mathematical model.

3.2. State Space Modelling

For further analysis, the mathematical model of the system should be translated into the state space model. The general form of a system state space is shown in Fig. 3[36].

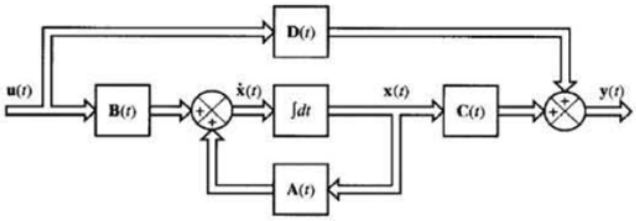

Fig. 3. Open Loop System Representation in State Space Equation

State space representation equation can be expressed as

$$\dot{\mathbf{x}} = \mathbf{Ax} + \mathbf{Bu} \quad (35)$$

$$\mathbf{y} = \mathbf{Cx} + \mathbf{Du} \quad (36)$$

where n is the total number of the state variables and x$\in \mathbb{R}^n$ is a state vector. $\dot{x}$ is the time derivative of the state vector.[36]

A vector u $\in \mathbb{R}^k$ is the control vector or control input which has k elements of control variables. The matrices A$\in \mathbb{R}^{n\,x\,n}$, B$\in \mathbb{R}^{n\,x\,k}$ and C $\in \mathbb{R}^{p\,x\,n}$ are named the system, the output and the input matrices, successively, where ppp is the output number.[36] The output vector is declared as y$\in \mathbb{R}^p$

For the case of the cart inverted pendulum system, the state vector, the derivative of the state vector and the input of the state vector are declared as $x=[x\ \theta\ \dot{x}\ \dot{\theta}]^T$, $\dot{x}=[\dot{x}\ \dot{\theta}\ \ddot{x}\ \ddot{\theta}]^T$,$u=v_a$,. In this case, the total number of the state variables is n=4. Arranging Eq. (40) and Eq. (43) into the state space form, the system matrices obtained as follows[36]:

$$\mathbf{A} = \begin{bmatrix} 0 & 0 & 1 & 0 \\ 0 & 0 & 0 & 1 \\ 0 & -\frac{mg}{M} & -\frac{c_1}{M} & 0 \\ 0 & \frac{(M+m)g}{Ml} & \frac{c_1}{Ml} & 0 \end{bmatrix},$$

$$\mathbf{B} = \begin{bmatrix} 0 \\ 0 \\ \frac{c_2}{M} \\ -\frac{c_2}{Ml} \end{bmatrix}, \mathbf{C} = \begin{bmatrix} 1 & 0 & 0 & 0 \\ 0 & 1 & 0 & 0 \end{bmatrix}$$

$$\mathbf{y} = [x\ \theta]^T, \mathbf{D} = \emptyset$$

Only x and θ can be observed directly from sensors in assumption, in the sense that the observed value from the sensor is the actual value. In practical, the conversion from the actual to the value that is used for the computation is required.[36]

3.3. The Pole Placement Method

The open–loop dynamics are determined by the characteristic polynomial of the matrix A:

$$|sI - A| = s^n + a_1 s^{n-1} + \cdots + a_{n-1}s + a_n \quad (37)$$

The coefficients a_i correspond to the current locations of the system poles.

A. Specify the desired closed-loop poles

From the design requirements on transient response such as settling time, overshoot, and damping - we choose an appropriate set of desired closed-loop poles $\mu_1,\ldots,\mu_n$. These poles define a new characteristic polynomial:

$$\prod_{i=1}^{n}(s - \mu_i) = s^n + \alpha_1 s^{n-1} + \cdots + \alpha_{n-1}s + \alpha_n \quad (38)$$

The coefficients α_i are the target coefficients that the closed-loop characteristic polynomial should attain.

B. Transform the system to controllable canonical form

Assume that the pair (A, B) is controllable. Then there exists a change of state variables $x=T_z$ such that the transformed pair (A_c, B_c) is in controllable canonical form. The transformation matrix T is constructed from the controllability matrix $C= [B\ AB \ldots A^{n-1}B]$ and an auxiliary companion-type matrix W derived from the coefficient a_i:

$$\mathcal{T} = \mathcal{C}\mathcal{W} \quad (39)$$

Using the matrix A and B, the controllability matrix can be calculated as $\mathcal{C}$ = [B AB A^2B A^3B]. Using the following parameters (M=1 kg, m=0.1 kg, l=0.25 m, r_l=0.015 m, R_a=1 Ω, K_t=K_b=0.02),

$$\mathcal{C} = \begin{bmatrix} 0 & 1.3333 & -2.3704 & 9.407 \\ 0 & -5.3333 & 9.4815 & -246.8293 \\ 1.3333 & -2.3704 & 9.4407 & -26.0752 \\ -5.3333 & 9.4815 & -246.8293 & 475.9751 \end{bmatrix}$$

Therefore, rank($\mathcal{C}$) = 4, confirming that the linearized system is fully controllable.

C. Compute the state-feedback gain matrix

In the z-coordinates, with A_c in companion form, the feedback gain vector in controllable canonical form can be obtained directly from the difference between the desired coefficients α_1 and the original coefficients a_i. Transforming back to the original coordinates yields the state-feedback gain

$$K = [\alpha_n - a_n,\ \alpha_{n-1} - a_{n-1},\ \ldots,\ \alpha_2 - a_2,\ \alpha_1 - a_1]\,T^{-1} \quad (40)$$

With the control law u=−Kx, the closed-loop matrix A_{cl} = A−BK has the characteristic polynomial given by (35). In other words, all closed-loop poles are placed exactly at the prescribed locations μ_i chosen in A.[36]

In tracking problems, a static input pre–compensator can be included so that

$$u=Nr-Kx \quad (41)$$

where the scalar (or diagonal) gain *N* is selected to achieve the desired steady-state accuracy for a step reference. The overall state–feedback closed-loop structure with this pre–gain is illustrated in Fig. 4.

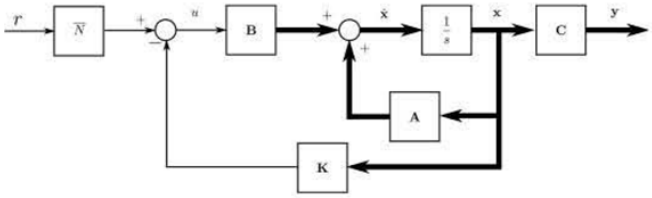

Fig. 4. Closed loop system with pre-gain

4. Result and discussion

To verify the effectiveness of the proposed control method, simulations have been performed in MATLAB. The parameters of the CIP system were determined as depicted in Table 1.

Table 1. The CIP parameters.

Parameters	Value	Unit
Armature resistance	1	Ω
Motor torque constant	0.02	Nm/A
Back emf constant	0.02	Vs/rad
Motor pulley radius	0.015	m
Pendulum mass	0.1	kg
Cart mass	1	kg
Pendulum rod length	0.25	m
Gravitational acceleration	9.81	m/s^2

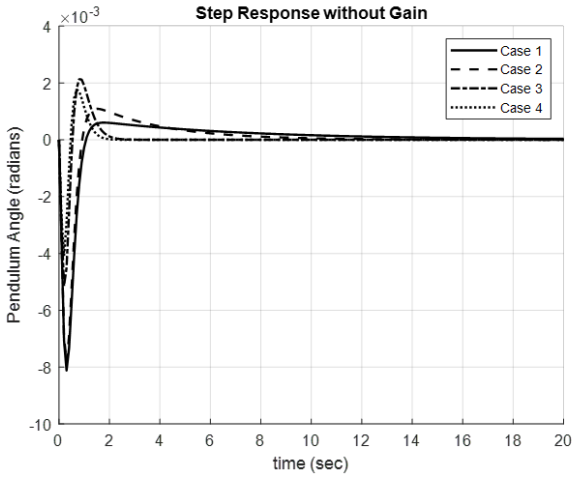

Fig. 5. Pendulum angle response

Fig. 5 shows the open-loop angle θ(t) after a smalldisturbance from the upright position. The pendulum quickly tips over and its angle grows roughly exponentially until it hits mechanical limits, confirming that the linearized CIP has an unstable pole in the right-half plane. This baseline clearly illustrates that, without feedback, the

system cannot maintain balance and motivates the use of a pole-placement controller.

Fig. 6 shows the corresponding cart motion x(t). As the pendulum falls, the reaction forces cause the cart to accelerate away from x(0) = 0, often moving more than 1 m in a few seconds with a roughly parabolic trajectory. Thus, the controller must both balance the pendulum and bring the cart position back to its reference using only one control input.

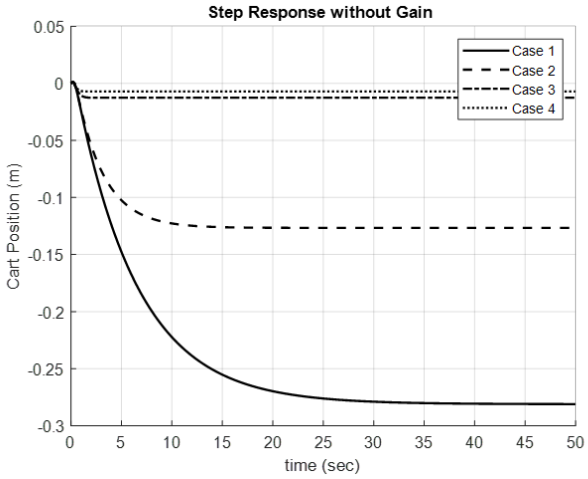

Fig. 6. Cart position response

Fig. 6 shows the closed-loop pendulum angle when the state-feedback law $u=-Kx$ (designed by pole placement) is applied. In contrast to the unstable open-loop case, the angle now returns smoothly to zero, with rise time about 0.5 s, settling time around 1.5 s, and overshoot near 15%, all determined by the chosen pole locations. Selecting dominant poles with damping ratio $\zeta \approx 0.7$ gives a good compromise between speed and oscillation, and the steady-state error is practically zero. This plot visually confirms that shifting the system poles to the left-half plane via state feedback stabilizes the CIP and achieves pendulum balancing.

Fig. 7 shows the closed-loop cart position, highlighting that the controller also achieves position regulation. Instead of drifting away as in the open-loop case, the cart first moves in one direction to help arrest the pendulum's fall, then smoothly returns to x=0. Its settling time, typically around 3–4 s, is longer than that of the pendulum angle, reflecting the energy exchange and the compromise of controlling both states with a single actuator. The negligible steady-state error confirms that the coupled dynamics are well handled. By shifting the poles linked to the cart dynamics further left the return to the origin could be made faster, though at the cost of higher control effort.

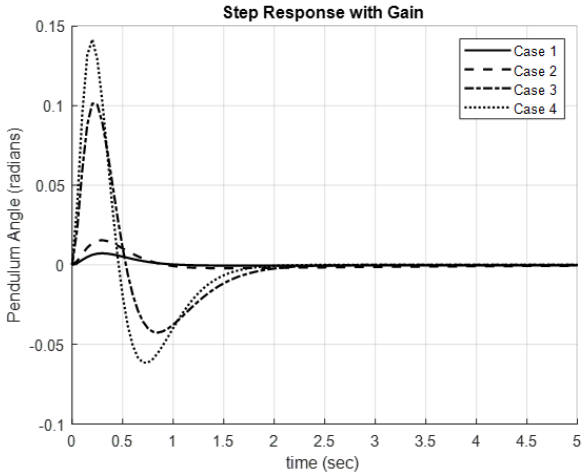

Fig. 7. Pendulum angle response with gain.

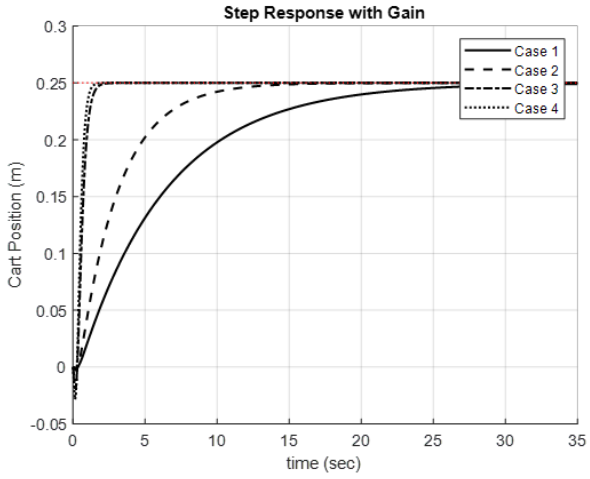

Fig. 8. Cart position response with gain.

5. Conclusion

This work addressed the stabilization problem of the underactuated and inherently unstable CIP system with the pole placement method. By linearizing the nonlinear dynamics around the upright equilibrium and verifying system controllability, a state-feedback controller was systematically designed through the selection of desired closed-loop pole locations. The resulting gain matrix successfully stabilized both the pendulum angle and cart position. Extensive MATLAB/Simulink simulations confirmed the controller's effectiveness, demonstrated the tunability of transient performance via pole assignment, and highlighted the associated control-effort trade-offs.

The study contributes: (i) a clear derivation of the linearized state-space model; (ii) a complete pole-placement-based stabilization procedure; and (iii) numerical validation demonstrating reliable closed-loop

performance. Future work will focus on observer-based output feedback, robustness enhancement, hardware-in-the-loop implementation, and extending the methodology to more complex underactuated systems.

References

[1] S. Mahmoudi Rashid, A. Rikhtehgar Ghiasi, and S. Ghaemi, "A new distributed robust H∞ control strategy for a class of uncertain interconnected large-scale time-delay systems subject to actuator saturation and disturbance," Journal of Vibration and Control, vol. 31, no. 13–14, pp. 2651–2675, Jul. 2024, doi: 10.1177/10775463241259345.

[2] V. T. Duong, C. T. Truong, T. T. Nguyen, H. H. Nguyen, and T. T. Nguyen, "State space model identification using model reference adaptive approach: software and hardware-in-the-loop simulation," Cogent Eng, vol. 11, no. 1, 2024, doi: 10.1080/23311916.2024.2434938.

[3] Nhut Thang Le, Cong Toai Truong, Huy Hung Nguyen, Tan Tien Nguyen, and Van Tu Duong, "Position Tracking Control of a Permanent Magnet Steering Wheel Equipped to a Vertical Tank Robot: From Theory, Simulation to Practice," Measurement and Control, pp. 1–18, 2025, doi: 10.1177/00202940251372834.

[4] Nhut Thang Le, Minh Tri Nguyen, Cong Toai Truong, Van Tu Duong, and Huy Hung Nguyen, "Recursive Least Squares Algorithm for Online Parameter Identification of DC Motor: Theory and Practice," in 10th International Conference on Engineering and Emerging Technologies, Dubai: IEEE, Dec. 2024, pp. 27–28. doi: 10.1109/ICEET65156.2024.10913584.

[5] N. T. Le et al., "Development of a Multi-Suspension Unit for Solar Cleaning Robots to Mitigate Vibration Impact on Photovoltaic Panels," Applied Sciences (Switzerland), vol. 13, no. 22, Nov. 2023, doi: 10.3390/app132212104.

[6] M. T. Nguyen, C. T. Truong, V. T. Nguyen, V. T. Duong, H. H. Nguyen, and T. T. Nguyen, "Research on Adhesive Coefficient of Rubber Wheel Crawler on Wet Tilted Photovoltaic Panel," Applied Sciences (Switzerland), vol. 12, no. 13, Jul. 2022, doi: 10.3390/app12136605.

[7] N. T. Le, C. T. Truong, H. H. Nguyen, T. T. Nguyen, and V. T. Duong, "Yaw angle determination of a mobile robot operating on an inclined plane using accelerometer and gyroscope," Measurement, vol. 247, p. 116806, 2025, doi: 10.1016/j.measurement.2025.116806.

[8] N. T. Le et al., "Development of Two-Axes Gimbal System Testing Platform for Validating Tilt Sensor Precision," in Recent Advances in Electrical Engineering and Related Sciences: Theory and Application, Singapore: Springer Nature Singapore, 2025, pp. 203–209. doi: 10.1007/978-981-96-4573-2_17.

[9] C. T. Truong et al., "Model identification of ventilation air pump utilizing Ridge-momentum regression and Grid-based structure optimization," Mathematical Biosciences and Engineering 2025 8:2020, vol. 22, no. 8, pp. 2020–2038, 2025, doi: 10.3934/MBE.2025074.

[10] D. K. Nguyen, C. T. Truong, V. T. Duong, H. H. Nguyen, and T. T. Nguyen, "Model identification of two double-acting pistons pump," Journal of Advanced Marine Engineering and Technology, vol. 47, no. 2, pp. 59–65, Apr. 2023, doi: 10.5916/jamet.2023.47.2.59.

[11] Cong Toai Truong et al., "Model Identification of Two Double-Acting Pistons Pump A NARX Network Approach," in International Conference on Ubiquitous Robots, 2023. doi: 10.1109/UR57808.2023.10202388.

[12] Trung Dat Phan, Ly Xuan Truong Pham, Cong Toai Truong, Van Tu Duong, and Huy Hung Nguyen, "Adaptive Sliding Mode Control for a Blower-Based Breathing Simulator with Unknown and Time-Varying Airway Resistance and Compliance," in 10th International Conference on Engineering and Emerging Technologies, Dubai: IEEE, Dec. 2024, pp. 27–28. doi: 10.1109/ICEET65156.2024.10913788.

[13] Cong Toai Truong, Kim Hieu Huynh, Van Tu Duong, Huy Hung Nguyen, Le An Pham, and Nguyen Tan Tien, "Model free volume and pressure cycled control of automatic bag valve mask ventilator," AIMS Bioeng, pp. 192–207, 2021, doi: 10.3934/bioeng.2021017.

[14] Cong Toai Truong, Kim Hieu Huynh, Van Tu Duong, Huy Hung Nguyen, Le An Pham, and Tan Tien Nguyen, "Linear regression model and least square method for experimental identification of AMBU bag in simple ventilator," International Journal of Intelligent Unmanned Systems, vol. 11, no. 3, pp. 378–395, Jun. 2023, doi: 10.1108/IJIUS-07-2021-0072.

[15] S. Ren, L. Han, J. Mao, and J. Li, "Optimized Trajectory Tracking for Robot Manipulators with Uncertain Dynamics: A Composite Position Predictive Control Approach," Electronics (Switzerland), vol. 12, no. 21, Nov. 2023, doi: 10.3390/electronics12214548.

[16] L. Author et al., "Design and Implementation of Pole Placement Controllers," IEEE Access, vol. 8, pp. 11245–11256, 2020.

[17] N. Author et al., "MATLAB-Based Simulation of Inverted Pendulum Systems," Simulation Modelling Practice and Theory, vol. 96, 2020.

[18] O. Author and P. Author, "Trade-Off Analysis in Pole Placement Control Design," Journal of Dynamic Systems, Measurement, and Control, vol. 142, 2020.

[19] M. Rani and S. S. Kamlu, "Optimal LQG controller design for inverted pendulum systems," *Scientific Reports*, 2025

[20] S. Engelsman and F. Klein, "Inertial-based LQG control: A new look at inverted pendulum stabilization," arXiv:2503.18926, 2025

[21] S. Farkhooi, *Embedded model predictive control of the Furuta pendulum*, M.S. thesis, Dept. Information Technology, Uppsala Univ., Uppsala, Sweden, 2025

[22] D.-B. Pham, Q.-T. Dao, and T.-V.-A. Nguyen, "Optimized hierarchical sliding mode control for the swing-up and stabilization of a rotary inverted pendulum," *Automation*, vol. 5, no. 3, pp. 282–296, 2024

[23] S. Adamiat, W. Kouw, B. van Erp, and B. de Vries, "Message passing-based Bayesian control of a cart-pole system," in *Active Inference: 5th Int. Workshop, IWAI 2024*, 2024, pp. 209–221

[24] D. Ju, J. Lee, and Y. S. Lee, "Transition control of a rotary double inverted pendulum using direct collocation and sim-to-real reinforcement learning," *Mathematics*, vol. 13, no. 4, art. 640, 2025

[25] ME C134 / EE C128 Course Staff, *Lab 6a: Pole placement for the inverted pendulum*, Univ. of California, Berkeley, Berkeley, CA, USA, course notes, 2018

[26] S. Sawant, A. S. Anand, D. Reinhardt, and S. Gros, "Learning-based MPC from big data using reinforcement learning," arXiv:2301.01667, 2023

[27] A. B. Kordabad, D. Reinhardt, A. S. Anand, and S. Gros, "On the improvement of model-predictive controllers," preprint, 2023

[28] G. Rigatos, M. Abbaszadeh, P. Siano, G. Cuccurullo, J. Pomares, and B. Sari, "Nonlinear optimal control for the rotary double inverted pendulum," *Advanced Control for Applications: Engineering and Industrial Systems*, vol. 6, no. 2, art. 140, 2024.

[29] Z. Ben Hazem, "Study of Q-learning and deep Q-network learning control for a rotary inverted pendulum system," *Discover Applied Sciences*, vol. 6, art. 49, 2024.

[30] D. Ju, T. Lee, and Y. S. Lee, "Implementation of 12 transition controls for rotary double inverted pendulum using direct collocation," in *Proc. 21st Int. Conf. on Informatics in Control, Automation and Robotics (ICINCO)*, Porto, Portugal, 2024, pp. 92–100.

[31] Z. Ben Hazem, "Study of Q-learning and deep Q-network learning control for a rotary inverted pendulum system," *Discover Applied Sciences*, vol. 6, art. 49, 2024.

[32] R. Hernandez, R. Garcia-Hernandez, and F. Jurado, "Modeling, simulation, and control of a rotary inverted pendulum: A reinforcement learning-based control approach.

[33] A. M. Al Juboori, M. T. Hussein, and A. S. G. Qanber, "Swing-up control of double-inverted pendulum systems," *Mechanical Sciences*, vol. 15, pp. 47–54, 2024.

[34] Y. Wang, H. Guo, S. Wang, L. Qian, and X. Lan, "Bootstrapped model predictive control," in *Proc. 13th Int. Conf. on Learning Representations (ICLR)*, Singapore, 2025.

[35] W. Acuña-Bravo, A. G. Molano-Jiménez, and E. Canuto, "Embedded model control for underactuated systems: An application to Furuta pendulum," *Control Engineering Practice*, vol. 113, p. 104854, 2021

[36] Indrazllo Siradjuddin et al., "Stabilising A Cart Inverted Pendulum System Using Pole Placement Control Method", *IEEE*, 2017.